Production and preservation of organic matter: The significance of iron

Stephen R. Meyers[1]

[1] "Iron fertilization" has been previously recognized as a potential mechanism for enhanced organic matter burial in marine sediments. However, the singular view of iron as a control on primary production overlooks its role in sedimentary diagenesis, a factor that must be evaluated when considering organic matter accumulation. This study examines the role of iron as a buffer of pore water sulfide and its implications for marine organic matter burial. Biogeochemical model experiments indicate that dissolved sulfide buildup in surficial marine sediments is highly sensitive to reactive iron concentration. A reduction in reactive iron concentration can initiate dissolved sulfide accumulation, the consequences of which include inhibition of bioturbation/bioirrigation, a decrease in oxygen exposure time, and enhanced organic matter burial. Alternatively, an increase in reactive iron concentration can serve to decrease organic matter burial. The coupling of iron and phosphorous cycling within marine sediments provides an important positive feedback, and therefore this mechanism is designated the "sulfide buffer/phosphorous trap hypothesis." Given sufficient organic carbon supply, carbonate-rich and opal-rich sediments should be especially prone to the development of sulfidic conditions because of a deficiency in terrigenous iron. Widespread chalk and marl deposition during the Cretaceous, in association with the evolutionary expansion of calcareous plankton, may have predisposed many benthic marine environments to the accumulation of toxic hydrogen sulfide and fostered the development of "oceanic anoxic events." Comparison of model results with proxy data from oceanic anoxic event II (middle Cretaceous) suggests a complex role of iron as a control on both organic matter production and preservation.

1. Introduction

[2] Over the past two decades iron has become established as an essential micronutrient that can limit primary production in large portions of the ocean [e.g., *Martin and Fitzwater*, 1988; *Martin et al.*, 1989; *Martin*, 1990; *Kolber et al.*, 1994; *Martin et al.*, 1994; *Behrenfeld et al.*, 1996; *Behrenfeld and Kolber*, 1999; *Boyd et al.*, 2000]. Numerous studies have shown that increased iron availability has important consequences for carbon and nitrogen cycling in marine ecosystems, including the enhancement of cyanobacterial nitrogen fixation [*Michaels et al.*, 1996; *Falkowski*, 1997], an increase in C:Si and N:Si uptake ratios in diatoms [*Hutchins and Bruland*, 1998; *Hutchins et al.*, 1998; *Firme et al.*, 2003], and a decrease in the amount CO_2 respired by heterotrophic bacteria (per a given quantity of organic carbon consumed; *Tortell et al.*, 1996]. Iron-limited conditions have been identified is such varied settings as the Southern Ocean, the Equatorial Pacific, and coastal margin upwelling systems [*Martin and Fitzwater*, 1988; *Martin et al.*, 1989; *Martin*, 1990; *Hutchins et al.*, 1998; *Firme et al.*, 2003; *Chase et al.*, 2005]. Given the numerous mechanisms by which iron can influence marine bioproductivity, and the large areas that are affected, changes in iron delivery to the oceans are expected to have a substantial impact on global organic matter production in surface waters, and the export of organic matter to the deep ocean [*Martin*, 1990; *Kumar et al.*, 1995; *Falkowski et al.*, 1998].

[3] In addition to its role in carbon and nitrogen cycle dynamics within the surface and deep oceans, iron fertilization provides a compelling mechanism for promoting organic matter burial in marine sediments [e.g., *Leckie et al.*, 2002; *Saltzman*, 2005]. For example, it has been suggested that the dramatic increase in organic carbon burial during mid-Cretaceous oceanic anoxic events (OAEs [*Schlanger and Jenkyns*, 1976; *Arthur et al.*, 1985]) is partially attributable to iron fertilization of primary production via enhanced hydrothermal activity [*Sinton and Duncan*, 1997; *Larson and Erba*, 1999; *Jones and Jenkyns*, 2001; *Leckie et al.*, 2002; *Erba*, 2004; *Snow et al.*, 2005]. If this proves to be the case, it is likely that an intensification of nitrogen fixation via increased iron delivery sustained high levels of primary production, even under elevated levels of denitrification during the events. In support of this hypothesis, the abundance of cyanobacterial membrane lipids during some of the mid-Cretaceous OAEs [*Kuypers et al.*, 2004], and the observation of bulk organic matter $\delta^{15}N$ values typical of newly fixed nitrogen [*Kuypers et al.*, 2004; *Meyers*, 2006], suggest a particularly important role for nitrogen fixers. Recent culture experiments

[1]Department of Geological Sciences, University of North Carolina at Chapel Hill, Chapel Hill, North Carolina, USA.

with cyanobacteria [*Junium et al.*, 2006] have spawned further insight on this issue: isotope fractionations observed in iron-enriched cultures are consistent with extremely light $\delta^{15}N$ values documented in some OAE II deposits (late Cenomanian–early Turonian). Further support for greater oceanic iron delivery during OAE II comes from an observed increase in iron accumulation, with a large fraction of the iron decoupled from the local terrigenous flux, consistent with a dissolved oceanic source [*Meyers et al.*, 2005].

[4] Although this evidence for a linkage between iron fertilization and organic matter burial is intriguing, when considering the transfer of organic carbon from the ocean to the lithosphere, it is essential to evaluate the role of iron in early diagenesis. Herein, I will investigate a diagenetic mechanism by which an increase in iron delivery can substantially decrease organic matter burial, particularly in continental margin sediments, the most significant marine environment for organic matter burial (~90% [*Hedges and Keil*, 1995]. This mechanism is dependent upon the role of iron in buffering dissolved sulfide via iron sulfidization [*Canfield*, 1989a; *Canfield et al.*, 1992; *Raiswell and Canfield*, 1996], and its implications for bioturbation/bioirrigation, oxygen exposure time, phosphorous cycling, and organic matter remineralization within surficial marine sediments. Ultimately, reactive iron concentration is the central feature of this biogeochemical hypothesis, which can be modulated by factors such as hydrothermal iron input, diagenetic iron remobilization, terrigenous iron flux (e.g., fluvial, aeolian supply) as well as biogenic dilution [*Raiswell*, 2006].

[5] A linkage between iron delivery, oxygen exposure time, and organic matter burial was previously proposed by *Meyers et al.* [2005]. A central question pertinent to this hypothesis is whether or not the kinetics of iron sulfidization are adequate to keep pace with sulfide production via sulfate reduction (can sulfide removal by this process compete with sulfide production?). Furthermore, what quantity of reactive iron is required to buffer sulfide buildup, and is this quantity geologically plausible? Finally, is reactive iron delivery (or more specifically concentration) variable enough over geologic timescales to function as a primary control on organic matter burial? In this study, I will evaluate these questions with biogeochemical model experiments and data from modern/ancient marine environments, and compare these results with geochemical burial flux estimates from one of the most globally extensive oceanic anoxic event intervals (OAE II) [*Schlanger and Jenkyns*, 1976; *Meyers et al.*, 2005]. Both model and data underscore a strong linkage between iron availability, oxygen exposure time and organic matter burial. Given these findings, it is apparent that the relationship between iron delivery and organic carbon burial in marine sediments can be complex, dependent upon the degree to which iron influences organic matter production ("iron fertilization") versus organic matter preservation.

2. Iron Diagenesis and the Sulfide Buffer/Phosphorous Trap Hypothesis

[6] Organic matter decomposition within marine sediments proceeds via a series of remineralization processes: aerobic decomposition, manganese reduction, iron reduction, nitrate reduction, sulfate reduction and methanogenesis [*Froelich et al.*, 1979]. Remineralization in each of these zones is dependent upon the reactivity and concentration of organic matter [*Berner*, 1980], and the concentration of the requisite terminal electron acceptor (e.g., O_2, NO_3^-, SO_4^{2-}). In addition, a variety of environmental factors (e.g., temperature, accumulation of toxic substances) affect metabolism, and therefore can play a role in controlling organic matter decomposition. For example, the upward diffusion of trace amounts of hydrogen sulfide into an overlying bioturbation zone can inhibit aerobic metabolism [*Wang and Chapman*, 1999], and thus can serve to diminish the sediment reworking and bioirrigation required to maintain oxidants such as NO_3^- and O_2 in pore waters [*Berner*, 1980].

[7] Owing to a sulfide limitation on the depth of bioturbation, factors that moderate sulfide levels in pore waters, such as the rate of sulfate reduction and the rate of sulfide mineralization, can potentially influence the thickness of the overlying remineralization zones. If iron delivery is sufficient to completely buffer sulfide production in surficial sediments via iron sulfidization [*Jorgensen*, 1977; *Canfield*, 1989a], active bioturbation/bioirrigation can expand the zone of aerobic degradation, and increase the exposure time of organic matter to oxygen. Since oxygen exposure time is strongly correlated to organic carbon burial efficiency [*Hartnett et al.*, 1998], elevated (reduced) iron delivery should serve to decrease (increase) organic carbon burial. Mechanistically, the observed relationship between oxygen exposure time and organic carbon burial efficiency may be a direct consequence of concomitant changes in the rate of delivery of organic matter to a hydrogen sulfide-rich environment, since hydrogen sulfide functions as a principal control on organic matter "hydrogenation," vulcanization, and preservation [*Sinninghe Damsté et al.*, 1989a, 1989b; *Sinninghe Damsté and de Leeuw*, 1990; *Adam et al.*, 1993; *Werne et al.*, 2000; *Hebting et al.*, 2006].

[8] Figure 1 displays a more detailed conceptual model for the biogeochemical linkage between reactive iron burial flux, bioturbation/bioirrigation, oxygen exposure time, phosphorous cycling and organic matter burial. A reduction in reactive iron delivery (Figure 1b) from an initial equilibrium state (Figure 1a) decreases the rate of pore water hydrogen sulfide removal via iron sulfidization, increasing pore water H_2S concentrations at depth, and increasing the rate of sulfide diffusion to overlying sediment pore waters. Elevated hydrogen sulfide flux to overlying sediments inhibits sediment reworking and bioirrigation, and sulfide oxidation further reduces pore water oxygen concentration [e.g., see *Jorgensen*, 1977]. These factors result in shoaling of the upper interface of the sulfate reduction zone (SRZ). Shoaling of this interface results in decreased exposure time of organic matter to oxygen (as well as other oxidants such as nitrate), and an increased flux of labile organic matter to the sulfate reduction zone, fueling enhanced rates of hydrogen sulfide production. The process creates a positive feedback, and results in continued shoaling of the sulfate reduction zone, potentially to the sediment-water interface (Figure 1c).

A) Equilibrium State 1
B) Decrease Reactive Iron Burial Flux
C) Equilibrium State 2
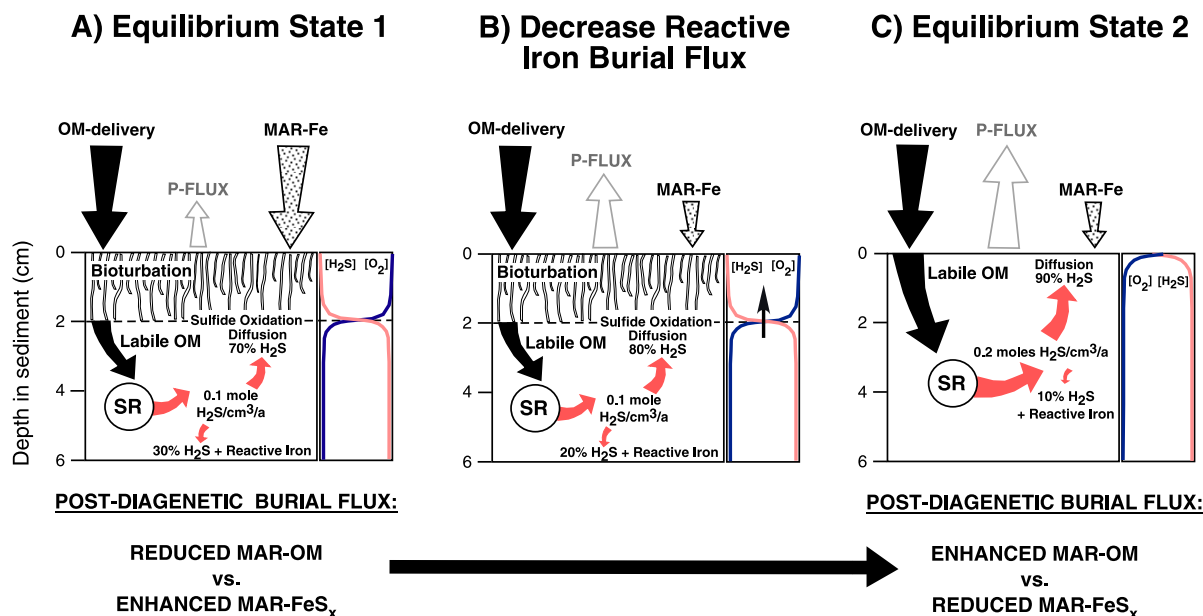
Figure 1. Proposed linkage between iron burial, hydrogen sulfide concentration, oxygen penetration depth, dissolved phosphorous flux, and organic matter burial (the "sulfide buffer/phosphorous trap hypothesis"). Arrow sizes reflect magnitudes of the fluxes. Definitions are OM, organic matter; SR, sulfate reduction; and MAR, mass accumulation rate. All fluxes are purely illustrative, intended to convey the basic premise of the hypothesis.

[9] There are two additional factors that can serve as positive feedbacks for this mechanism. First, high microbial Fe reduction (and Mn reduction) rates depend upon the availability of labile organic matter and Fe/Mn−oxides. Bioturbation provides a continuous supply of these reactants, and also permits the upward transport of solid phase Fe^{2+} (Mn^{2+}), which can subsequently be oxidized to Fe^{3+} (Mn^{4+}) and reused for microbial reduction and sulfide buffering [*Aller*, 1990; *Thamdrup and Canfield*, 1996]. Thus, if a decrease in reactive iron concentration drives hydrogen sulfide build up and a decrease in the degree of bioturbation/bioirrigation, this will serve to decrease organic matter remineralization due to Fe and Mn reduction, and will also decrease the sulfide buffering capacity.

[10] The coupling of iron and phosphorous cycling within sediments provides the final positive feedback. Since iron oxide particles within surface sediments serve as a trap for the remineralized phosphorous produced by organic matter decomposition, a decrease in the flux of iron oxides (Figure 1b) can potentially increase the phosphorous supply to overlying waters [*Krom and Berner*, 1980; *Slomp et al.*, 1996; *Cha et al.*, 2005]. In this regard, it is important to note that the iron phases most reactive to sulfidization (e.g., iron (oxyhydr)oxides [*Canfield et al.*, 1992]) are also those most effective at adsorbing phosphorous [*Ruttenberg*, 2003]. Finally, as sulfate reduction comes to dominate in the surface sediment, the preferential loss of phosphorous via anaerobic remineralization may serve to further increase phosphorous supply to the water column [*Ingall et al.*, 1993; *Van Cappellen and Ingall*, 1994]. These processes can potentially enhance primary production in surface waters, increasing the concentration of labile organic matter in the sediment, and thus drive higher rates of hydrogen sulfide production.

[11] Taken together, the processes outlined above will be referred to as the "sulfide buffer/phosphorous trap hypothesis," so as to emphasize the interaction of iron diagenesis with the sulfur and phosphorous cycles. The critical factor in this conceptual model is the concentration and reactivity of organic matter versus the concentration and reactivity of iron. Environmental conditions that promote increased hydrogen sulfide production (high concentrations of labile organic matter) and decreased hydrogen sulfide removal (lower reactive iron concentration) will yield more dramatic and rapid shoaling of the SRZ within the sediment. It has been proposed that such conditions are intrinsically associated with so-called "transgressive source rocks" [*Meyers et al.*, 2005].

[12] Section 3 investigates one aspect of the sulfide buffer/phosphorous trap hypothesis. Specifically, I explore the theoretical basis for the proposed relationship between iron burial, sulfide buffering, and oxygen exposure time using biogeochemical models and data from modern/ancient environments. As will be demonstrated, at low sediment burial rates relatively modest amounts of reactive iron can completely buffer hydrogen sulfide production in surficial sediments, even under high rates of primary production. These sediment burial rates are typical of many pelagic and continental margin environments, as well as many ancient source rocks [*Ibach*, 1982]. Thus changes in iron delivery to
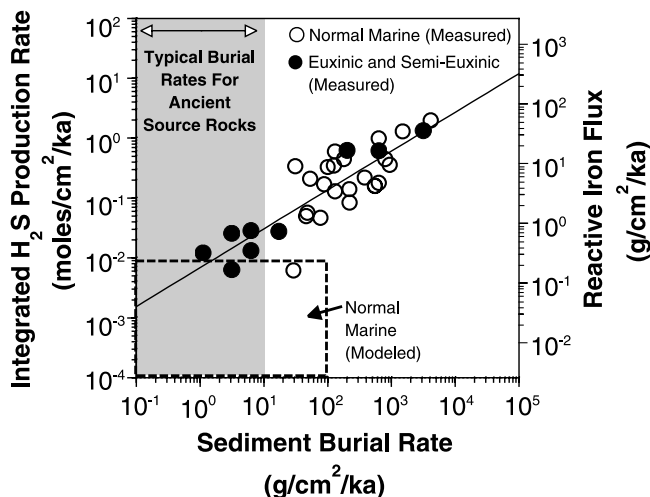
Figure 2. Integrated hydrogen sulfide production rates within the sediment versus sediment burial rates, based on sulfate reduction rates from *Canfield* [1989b]. The range of predicted production rates for normal marine sites with sediment burial rates <100 g cm^{-2} ka^{-1} is indicated by the dashed box [see *Canfield*, 1989b]. The *y* axis on the right side of the plot indicates the flux of reactive iron required to completely buffer the hydrogen sulfide produced in pore waters (as FeS$_2$, these values should be doubled for FeS). Burial rates for ancient source rocks are typically <10 g cm^{-2} ka^{-1} [*Ibach*, 1982].

such environments may function as an important control on organic matter burial.

3. Theoretical Considerations: Sulfate Reduction and Iron Sulfidization

[13] Sulfide production via sulfate reduction and sulfide removal by iron sulfidization serve as primary controls on pore water sulfide concentrations. The degree to which iron burial can buffer hydrogen sulfide accumulation in pore waters is primarily dependent on the quantity of iron and the kinetics of iron sulfidization, relative to the rate of hydrogen sulfide production via sulfate reduction. As demonstrated in numerous studies [*Berner*, 1980; *Canfield et al.*, 1992; *Poulton et al.*, 2004], sulfate reduction and iron sulfidization rates can be approximated using relatively simple kinetics. Sulfide production and removal by these processes can be modeled using organic carbon (G, dry wt %) and iron concentrations (C$_{Fe}$, dry wt %), the appropriate rate constants (k$_{org}$, a^{-1}; k$_{Fe}$, L$^{0.5}$mol$^{-0.5}$ a^{-1}), and the pore water hydrogen sulfide concentration (C$_{H2S}$, mol L^{-1}):

$$\text{sulfide production rate} = k_{org}G\left(\frac{\rho(1-\phi)}{\phi}\right)$$
$$\cdot\left(\frac{0.5}{12.01 \text{ gC/mol}}\right) \quad (1)$$

$$\text{sulfide removal rate} = -k_{Fe}C_{Fe}\left(\frac{\rho(1-\phi)}{\phi}\right)$$
$$\cdot\left(\frac{n_{H_2S}}{55.85 \text{ gFe/mol}}\right)(C_{H_2S})^{0.5} \quad (2)$$

[14] In these equations, ρ is the density of solids and φ is the sediment porosity. The term (0.5/12.01 g C mol^{-1}) is included in equation (1) to convert mass of carbon oxidized by sulfate reduction to moles of hydrogen sulfide produced (two carbons are oxidized per one sulfate consumed [*Berner*, 1980]). Likewise, the term (n_{H2S}/55.85 g Fe mol^{-1}) is included in equation (2) to convert mass of iron sulfidized to moles of hydrogen sulfide removed, where n_{H2S} is given a value of 1 for iron monosulfide (FeS) or 2 for pyrite (FeS$_2$). The most appropriate value for n_{H2S} depends on the timescale of interest, but generally should be intermediate between the values for FeS and FeS$_2$, as only a fraction of the reactive iron will be sulfidized to pyrite on relatively short timescales [*Canfield*, 1989a].

3.1. What Quantity of Reactive Iron (C$_{Fe}$) Is Required to Buffer Sulfide Buildup in Surficial Sediments, and Is This Quantity Geologically Plausible?

[15] In order to address this question, it is first necessary to examine the full range of sediment sulfate reduction rates that have been previously determined for modern euxinic to normal marine depositional environments. In Figure 2, the measured and modeled sulfate reduction rates of *Canfield* [1989b] have been plotted as equivalent sulfide production rates. This data set indicates an overall positive correlation between sulfide production and sediment burial rate, attributable to an increased rate of delivery of reactive (labile, high k$_{org}$) organic matter to the sediment sulfate reduction zone with increasing burial rate [*Canfield*, 1989b]. More generally, the impact of burial rate on sulfide production will be dependent upon the interplay of organic matter reactivity and concentration (see equation (1)). In this regard, the ultimate cause of increased burial rate is of critical importance. Increases in burial rate due to elevated organic matter delivery will serve to drive even higher rates of sulfide production. Alternatively, an increase in sediment burial rate due to elevated clay or carbonate flux will decrease the concentration of organic carbon (G), which can either increase or decrease the rate of sulfide production ("G × k$_{org}$"), depending upon concomitant changes in organic matter reactivity (k$_{org}$; see equation (1)). Although the large-scale trend in Figure 2 is clear, these factors account for data scatter observed at individual sediment burial rates. Of particular importance to the present discussion, if the general relationship observed in Figure 2 is appropriate for ancient marine environments, the low burial rates associated with many source rocks [*Ibach*, 1982] indicate low rates of hydrogen sulfide production in the sediment. Under such conditions, hydrogen sulfide accumulation should be particularly sensitive to buffering by reactive iron.

[16] To determine the concentration of iron (C$_{Fe}$, see equation (2)) sufficient to buffer against sulfide accumula-

Wt.% Reactive Iron
required to buffer H$_2$S accumulation
assuming all iron sulfidized to FeS

Wt.% Reactive Iron
required to buffer H$_2$S accumulation
assuming all iron sulfidized to FeS$_2$
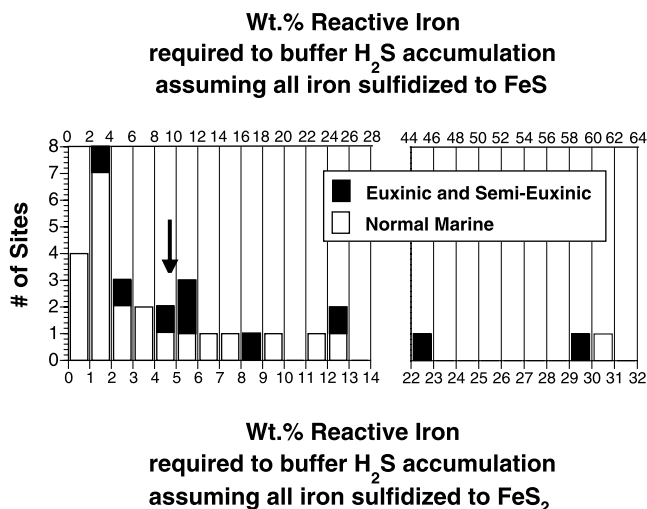
Figure 3. Histogram of wt % reactive iron required to completely buffer hydrogen sulfide production in pore waters as FeS (top scale) or FeS$_2$ (bottom scale), calculated for the euxinic, semieuxinic, and normal marine sites in Figure 2. The arrow indicates the iron concentration of the world average shale (4.7% [*Turekian and Wedepohl*, 1961]).

tion, the integrated hydrogen sulfide production rates in Figure 2 are transformed into theoretical reactive iron fluxes (right side of plot in Figure 2) assuming all hydrogen sulfide reacts to form either FeS or FeS$_2$, with no diffusive loss. This is an extremely conservative approach, as some fraction of the sulfide typically escapes the sediment via diffusion (between ~20% and 94% [*Jorgensen*, 1977; *Berner*, 1985; *Chanton et al.*, 1987]). These theoretical reactive iron fluxes are divided by the measured sediment burial rate to estimate the required weight percent reactive iron (C$_{Fe}$). The results (Figure 3) indicate that small concentrations of iron (e.g., less than the world average shale value of 4.7% [*Turekian and Wedepohl*, 1961]) are commonly sufficient to buffer against hydrogen sulfide accumulation in pore waters, regardless of whether the iron is completely sulfidized to pyrite or to an intermediate monosulfide phase.

[17] It is important to note that the results in Figure 3 do not consider the variable reactivities of different iron minerals (k$_{Fe}$ in equation (2); see section 3.2), nor the hydrogen sulfide produced in euxinic water columns. Given this additional hydrogen sulfide reservoir, a portion of the reactive iron will be sulfidized prior to reaching the sediment. For example, in the modern Black Sea most of the available reactive iron is sulfidized within the water column [*Lyons*, 1997]. As will be further discussed in section 3.4, euxinic systems have an iron biogeochemistry that is unique in some regards. For the sake of the present discussion, however, the estimates in Figure 3 are most appropriate when a stable stratified euxinic water column is absent, consistent with the interpretation of many ancient organic-rich strata [e.g., *Sageman*, 1989; *Arthur and Sageman*, 1994; *Murphy et al.*, 2000; *Sageman et al.*, 2003; *Meyers et al.*, 2005]. In summary, we can conclude that relatively

modest quantities of iron should be sufficient to buffer pore water hydrogen sulfide accumulation in many modern environments, if the kinetics of iron sulfidization are fast enough to keep pace with sulfide production.

3.2. Is the Kinetics of Iron Sulfidization Adequate to Keep Pace With Sulfide Production via Sulfate Reduction?

[18] Whether or not pore water sulfide buffering will occur at a rate sufficient to compensate for sulfide production is dependent upon the kinetics of iron sulfidization, relative to the kinetics of hydrogen sulfide production. Rate constants for sulfate reduction (k$_{org}$ in equation (1)) have been determined by *Toth and Lerman* [1977], and display a sedimentation rate dependence similar to the integrated sulfide production rates shown in Figure 2. Rate constants for iron sulfidization (k$_{Fe}$ in equation (2)) have also been determined for numerous iron-bearing minerals and display a wide range of reactivity [*Canfield et al.*, 1992; *Raiswell and Canfield*, 1996; *Poulton et al.*, 2004], with (oxyhydr)oxides characterized by the largest k$_{Fe}$ values (half-lives on the order of minutes to days), while poorly reactive minerals (e.g., sheet silicates) are characterized by half-lives of up to 2 million years (a) [*Raiswell and Canfield*, 1996; *Poulton et al.*, 2004]. These k$_{org}$ and k$_{Fe}$ values have been employed in equations (1) and (2) to estimate rates of hydrogen sulfide production and removal at the top of the sulfate reduction zone, where
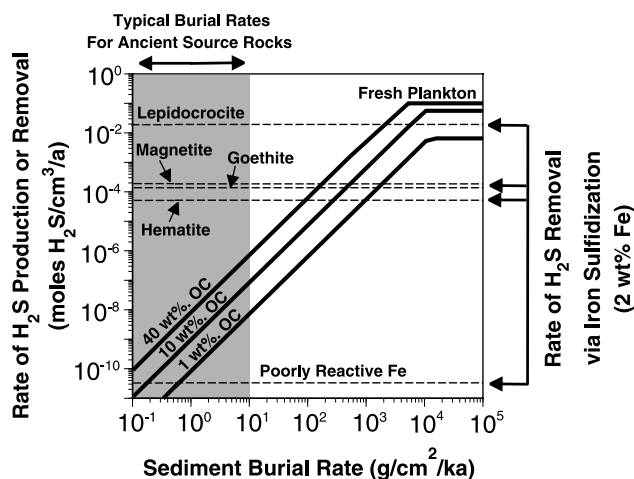
Figure 4. Pore water H$_2$S production rates (solid lines) and rates of H$_2$S removal via FeS formation (dashed lines, rates should be doubled for FeS$_2$). H$_2$S production rates are determined for sediments with organic carbon concentrations of 1 wt %, 10 wt %, and 40 wt % (theoretical maximum). The first-order rate constant for decomposition of fresh plankton [*Westrich and Berner*, 1984] is employed as a maximum value for organic matter remineralization via sulfate reduction. H$_2$S removal via sulfidization of each highly reactive iron phase utilizes an iron concentration of 2 wt % and an initial H$_2$S concentration of 0.1 mM. The calculations for poorly reactive iron do not include an explicit term for initial H$_2$S concentration, as rate constants incorporating this dependence are not yet available. Model details are outlined in the text and in Appendix A.

both terms should be maximized (Figure 4 and Appendix A). For the sake of the immediate discussion, it is assumed that sulfide production and removal rates at depth in the SRZ will decrease proportionally, although this issue will be explicitly addressed in section 3.3.

[19] The results in Figure 4 are calculated using a modest iron concentration of 2 wt %, a hydrogen sulfide concentration of 0.1 mM, and an n_{H2S} value of one (i.e., iron sulfidization to FeS; multiply the results by a factor of two for FeS_2). The rate of hydrogen sulfide removal for all of the iron (oxyhydr)oxide phases exceeds the rate of sulfide production when sediment burial rates are low (<100 g cm^{-2} ka^{-1}). This is true even at the highest theoretical organic carbon (OC) concentration of 40 wt %, which should reflect the highest possible level of primary production. At very low sediment burial rates (<0.5 g cm^{-2} ka^{-1}), even poorly reactive iron may function as an important sulfide buffer. Given these results, we would expect that hydrogen sulfide accumulation in the uppermost sediments should be completely buffered via iron sulfidization when sediment burial rates are low, unless the iron concentration is substantially reduced below 2 wt %, or an euxinic water column is present (providing an additional hydrogen sulfide reservoir for reactive iron depletion).

[20] Figure 5 illustrates the strong dependence of iron sulfidization on the initial concentration of both hydrogen sulfide and reactive iron (see equation (2)). There are two important concepts exemplified in this analysis. First, as hydrogen sulfide concentration increases within pore waters, each of the iron phases becomes more effective at buffering against further hydrogen sulfide accumulation. Second, since the concentration of reactive iron in a given sediment layer must decrease as iron sulfidization proceeds, the buffering capacity must also diminish (Figure 5d shows an example of such a trajectory for a sediment layer undergoing burial). At steady state, this decreased buffering capacity will be accompanied by a decrease in hydrogen sulfide production rate, because of decreased lability and concentration of organic matter with depth. The relative changes in the magnitudes of these two processes during sediment burial will dictate whether or not hydrogen sulfide accumulates substantially at depth (this topic is dealt with in greater detail in section 3.3). However, the results in Figure 5d suggest that even trace amounts of hematite iron (e.g., less than 0.1 wt %) can be sufficient to remove hydrogen sulfide more quickly then it is produced, but only when sediment burial rates are low (see Figure 4 for H$_2$S production rates). Once the most reactive phases are depleted at depth, ''poorly reactive'' iron can have a substantial role in controlling pore water sulfide levels [*Raiswell and Canfield*, 1996] (also see section 3.3). In summary, this analysis of the kinetics of sulfide production and removal indicates that iron sulfidization is rapid enough to remove sulfide as quickly as it is produced, but this will critically depend upon the specific iron mineralogy, its concentration, and the sediment burial rate.

3.3. A Pore Water Sulfide Model

[21] A more sophisticated pore water sulfide model (see Appendix B for details) adapted from *Raiswell and Canfield*

[1996] is utilized to further explore the linkage between iron burial, sulfide buffering and oxygen exposure time. Figure 6 illustrates changes in pore water sulfide concentration within the upper meter of modeled sediment, given a range of organic carbon and iron concentrations. The model utilizes the same rate constants (k_{org}, k_{Fe}) and depositional parameters (e.g., sedimentation rate of 5 cm ka^{-1}) employed by *Raiswell and Canfield* [1996] in their examination of Peru Margin sediments. The analysis is restricted to poorly reactive iron (see Figure 4), since the model was originally developed to investigate this phase and has been shown to produce reliable results.

[22] A fundamental requirement of the hypothesis outlined in Figure 1 is that changes in iron sulfidization rates are sufficient to impact bioturbation depth. Thus interpretation of the results in Figure 6 is dependent upon an understanding of the relationship between dissolved sulfide concentration and sediment toxicity. Although precise sulfide toxicity levels for marine benthos are limited, for the sake of illustration Figure 6 identifies the sulfide level that yields 50% mortality in the marine polychaete *Nereis* given a 24-h exposure time (5.76 mg L^{-1} [*Vismann*, 1990; *Wang and Chapman*, 1999]). If the sulfide tolerance of these infaunal Polychaetes is typical of most pelagic and hemipelagic benthos, the model results suggest that decreases in iron concentration by several wt % should dramatically impact the depth of bioturbation (Figure 7), altering oxygen exposure time by $10^3 - 10^6$ a in slowly accumulating sediments such as those modeled here (sedimentation rate = 5 cm ka^{-1}). Since a decrease in iron content causes sulfide buildup and results in shoaling of the depth of sulfide toxicity (and therefore bioturbation; compare the 6% Fe and 1% Fe in Figures 6 and 7), the concentration of organic carbon reaching the sulfate reduction zone also increases because of decreased aerobic and dysaerobic remineralization, yielding further shoaling of the SRZ (see the 10% OC profile in Figure 6). As noted earlier, this creates a positive feedback, with continued shoaling of the upper interface of the sulfate reduction zone, and has potential consequences for dissolve phosphorous flux to the water column.

3.4. Is Reactive Iron Concentration (C_{Fe}) Variable Enough on Geologic Timescales to Function as a Primary Control on Organic Matter Burial?

[23] The above analyses indicate the potential of reactive iron to influence pore water sulfide levels and oxygen exposure time. However, if reactive iron concentration is to function as an important control on organic matter burial, it must demonstrate a substantial degree of spatial/temporal variability. To evaluate this, Figure 8 presents iron concentration data from a range of modern marine environments, including oxic continental margin settings, oxic deep-sea settings, dysoxic environments and deep basin sediments of the euxinic Black Sea (as compiled by *Raiswell and Canfield* [1998, and references therein] and *Anderson and Raiswell* [2004, and references therein]). The data set is composed of three operationally defined iron fractions: total iron (Fe$_T$), highly reactive iron (F$_{HR}$) and poorly reactive iron (F$_{PR}$). Highly reactive iron includes FeS and FeS$_2$, in addition to the iron fraction that is extractable by dithionite
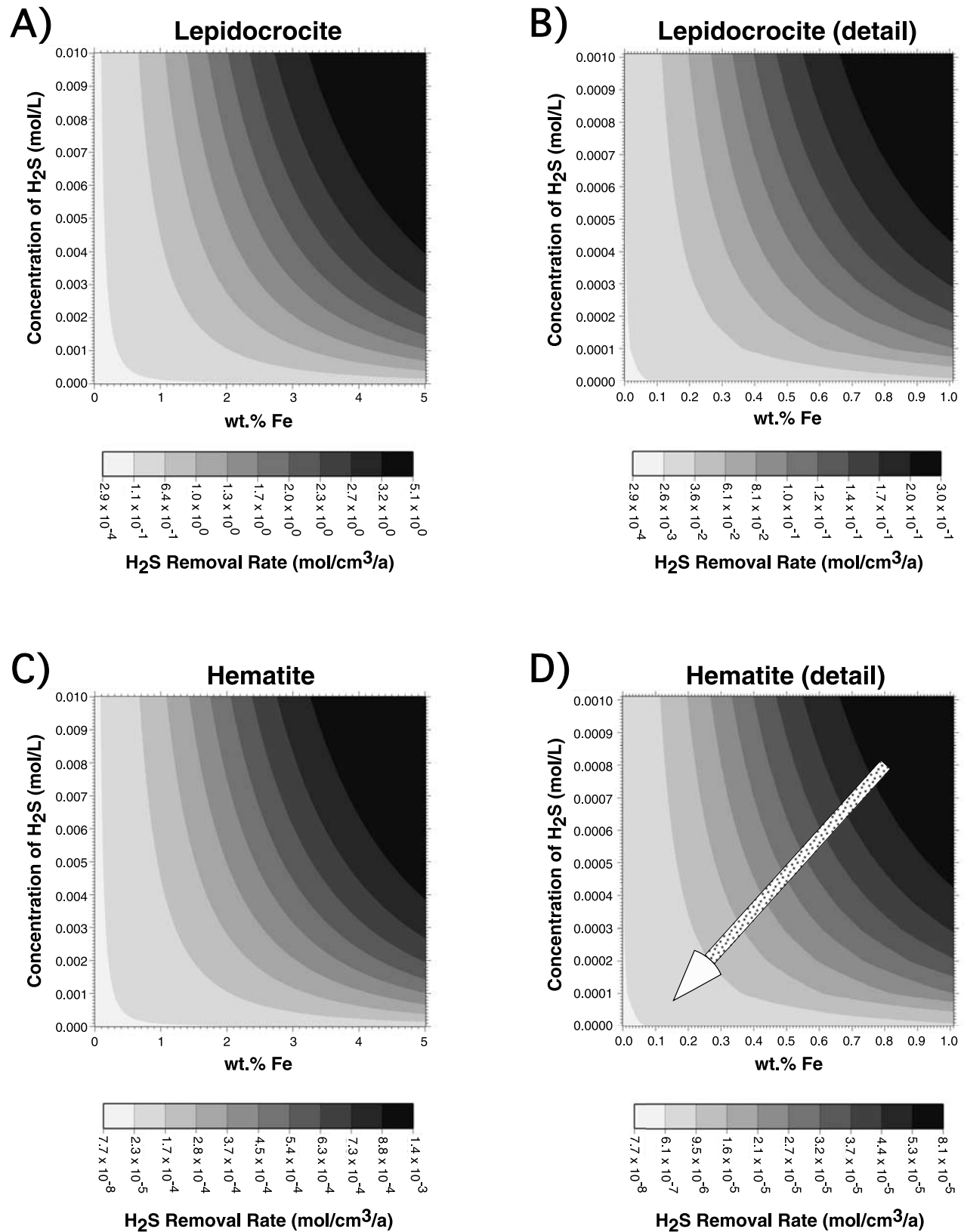
Figure 5. Biogeochemical model results displaying the dependence of iron sulfidization rate (as FeS, rates should be doubled for FeS_2) on the initial concentration of hydrogen sulfide and reactive iron: (a and b) lepidocrocite and (c and d) hematite. The arrow in Figure 5d illustrates progressive modification of a sediment layer undergoing burial.
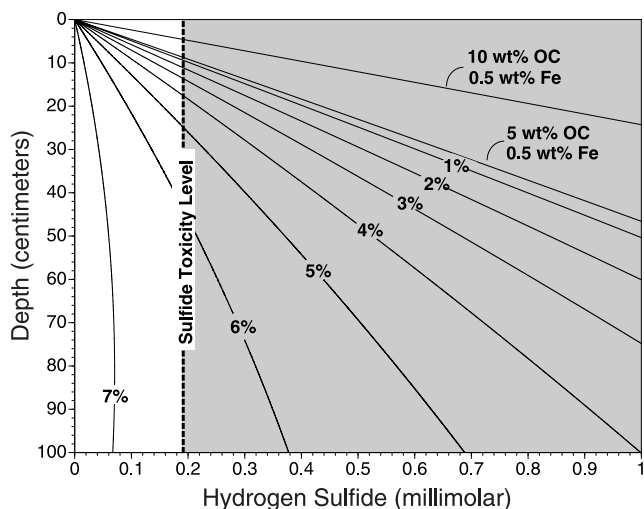
Figure 6. Pore water hydrogen sulfide concentrations calculated using the Peru Margin model of *Raiswell and Canfield* [1996]. Contours display sulfide profiles, given a range of Fe concentrations (0.5–7%) and an OC concentration of 5%. A sulfide profile for 10% OC and 0.5% Fe is also shown. The sulfide toxicity level is based on *Vismann* [1990] and *Wang and Chapman* [1999]. See Appendix B and the text for a detailed description of the model.

[*Raiswell and Canfield*, 1998]. Fe_{HR} is interpreted to represent iron originally present as (oxyhydr)oxides, as well as a small fraction of the silicate iron (the most reactive portion). Poorly reactive iron is operationally defined as the iron extractable by boiling HCl (Fe_{HCl}), less the highly reactive iron that is also extractable using this method (=$Fe_{HCl} - Fe_{HR}$) [*Raiswell and Canfield*, 1998]. Fe_{PR} is interpreted to represent the most poorly reactive silicate iron, sulfidized on timescales of millions of years.

[24] The iron data in Figure 8 demonstrate that oxic and dysoxic modern marine environments have a substantial degree of wt % Fe_{HR} and wt % Fe_{PR} variability. Two standard deviations (representing ~95% of the data) encompass a range of up to 1.8 wt % Fe_{HR} and 2 wt % Fe_{PR}. In contrast, although Black Sea deep basin sediments display comparable wt % Fe_{HR} variability, Fe_{PR} is nearly constant. The unique character of the Black Sea sediments is in part a consequence of an euxinic water column, which allows Fe^{2+} to be diagenetically mobilized from the shelf areas, transported laterally in the water column, and deposited as pyrite in the deep basin [*Canfield et al.*, 1996; *Lyons*, 1997; *Raiswell and Canfield*, 1998; *Wijsman et al.*, 2001; *Anderson and Raiswell*, 2004; *Lyons and Severmann*, 2006]. Additional factors that influence the character of iron in these Black Sea sediments may include an unusual highly reactive lithogenous fraction, and/or microbial transformation of poorly reactive iron (for further discussion see *Wijsman et al.* [2001], *Anderson and Raiswell* [2004], and *Lyons and Severmann*, 2006]).

[25] The concentration of reactive iron in ancient environments also displays substantial variability. For example, *Raiswell and Al-Biatty*'s [1989] analysis of normal marine sediments spanning the Cambrian to the Cretaceous identi-

fied reactive iron concentrations ($Fe_{HR} + Fe_{PR}$) ranging from less than 0.5 wt % to values in excess of 8 wt %. As another example, a detailed analysis of normal marine to euxinic sediments from the Devonian Appalachian Basin [*Sageman et al.*, 2003] documents a wide range of reactive iron concentrations ($Fe_{HR} + Fe_{PR}$), from 0.5 wt % to 7.92 wt %. However, it is important to note that highly enriched values in these Devonian data have been attributed to euxinic Fe scavenging [*Werne et al.*, 2002], as is presently observed in the Black Sea deep basin sediments.

[26] Previous studies have demonstrated that the fraction of reactive iron (Fe_{HR}/Fe_T and Fe_{PR}/Fe_T) within the modern sedimentary iron pool is remarkably consistent across normal marine environments [*Poulton and Raiswell*, 2002; *Anderson and Raiswell*, 2004]. This observation yields two important conclusions: (1) increases in wt % Fe_T should generally accompany increases in reactive iron concentration in normal marine environments, although the precise reactivity of the iron will depend upon mineralogy, and (2) biomineral dilution (or more generally, nonsiliciclastic dilution) functions as a particularly important control on reactive iron concentration. Regarding the first point, since the iron (oxyhydr)oxides are characterized by reactivities that can differ by orders of magnitude (Figure 4), more specific information on the distribution of these iron phases in modern (and ancient) environments is critical. New methods for the quantification of individual highly reactive phases show great promise for more precisely addressing this issue [*Poulton and Canfield*, 2005].

[27] With regards to the role of biomineral dilution in controlling reactive iron concentration, given sufficient organic carbon supply, carbonate-rich and opal–rich sediments should be especially prone to the development of sulfidic conditions. In general, elevated biomineral flux can simultaneously serve to decrease iron concentration, while increasing hydrogen sulfide production because of more rapid transport of labile organic matter into the zone of sulfate reduction (see Figure 2). This mechanism can poten-
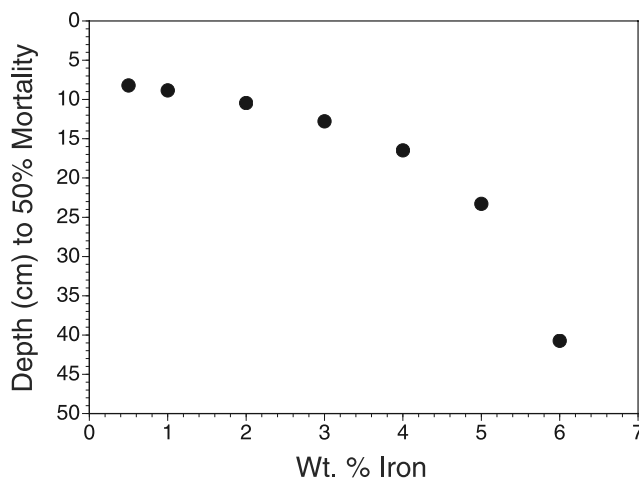
Figure 7. Weight percent iron within sediment versus the depth to sulfide-induced mortality (50%) for the marine polychaete *Nereis* [*Vismann*, 1990; *Wang and Chapman*, 1999], base on the model results in Figure 6.
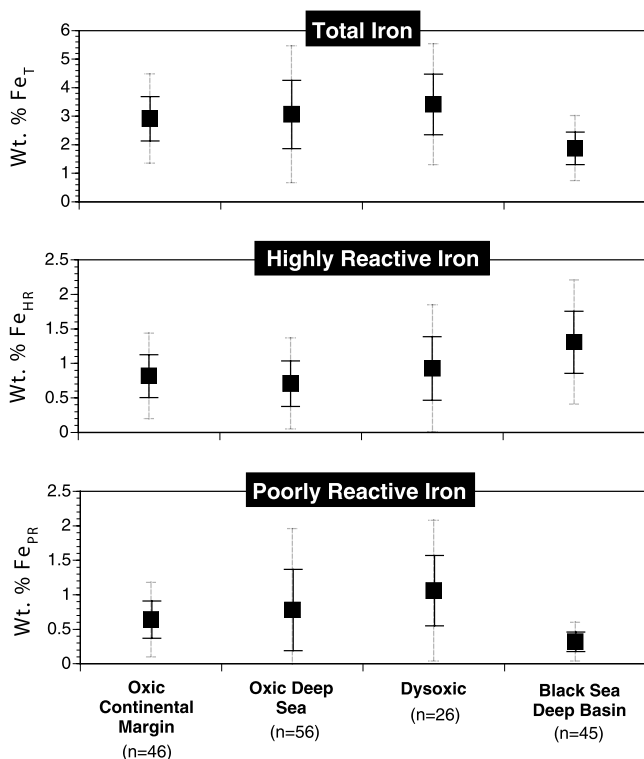
Figure 8. A compilation of iron concentration data [*Raiswell and Canfield*, 1998, and references therein; *Anderson and Raiswell*, 2004, references therein] from a range of modern marine environments, including oxic continental margin settings, oxic deep-sea settings, dysoxic environments, and deep basin sediments of the euxinic Black Sea. Squares represent mean values, solid lines indicate one standard deviation, and dotted lines indicate two standard deviations.

tially play in important role in organic matter burial in highly productive areas of the ocean. However, as mentioned previously (see sections 3.1) the relative impact of dilution flux on hydrogen sulfide production ("$G \times k_{org}$") critically depends upon its role in controlling organic carbon concentration (G) versus organic matter reactivity (k_{org}).

[28] Finally, given the capacity for skeletal dilution to regulate reactive iron concentration within sediments, evolutionary changes in pelagic biomineralization during the Phanerozoic may have played an important role in setting the stage for organic carbon burial events. For example, the deposition of vast amounts of iron-poor pelagic and hemipelagic chalk and marl during the Cretaceous, associated with the evolutionary expansion of foraminifera and calcareous nannoplankton [*Tappan and Loeblich*, 1973; *Premoli Silva and Sliter*, 1999], would have predisposed many benthic marine environments to the accumulation of toxic hydrogen sulfide. Diminished terrigenous iron delivery due to generally high eustatic sea level [*Haq et al.*, 1987], and consequent sequestration of terrigenous sediment within estuaries and flooded epicontinental seas, would have further exacerbated iron deficiency in many of these environments. Such secular biogeochem-

ical shifts may have fostered the development of global "oceanic anoxic events" during the Cretaceous, a situation already presaged by low oxygen concentration within the water column due to elevated temperature [e.g., see *Huber et al.*, 1995; *Schouten et al.*, 2003; *Jenkyns et al.*, 2004].

[29] On the basis of the results presented in sections 3.1–3.4 it is clear that changes in iron concentration within sediments can substantially impact sulfide concentrations in pore waters, thereby affecting the intensity of bioturbation/bioirrigation, oxygen exposure time, and organic matter burial. The role of iron in driving organic matter burial must therefore be dependent upon (1) the bioavailability of iron for bioproduction (estimated to be no greater than 40%, possibly <1% [*Jickells and Spokes*, 2001; *Wu et al.*, 2001; *Boyle et al.*, 2005] versus (2) its role in controlling the diagenetic remineralization processes outlined in section 2.

4. Role of Iron During Cretaceous Oceanic Anoxic Events: Production or Preservation?

[30] The Cretaceous is punctuated by several episodes of enhanced organic matter burial, known as oceanic anoxic events [*Schlanger and Jenkyns*, 1976]. Among these events, the late Cenomanian–early Turonian (C/T) OAE II is one of the most globally extensive, characterized by organic-rich sediments deposited in environments ranging from the deep sea to shallow epicontinental seaways [*Schlanger et al.*, 1987; *Jenkyns*, 1980]. The OAE II is distinguishable by a characteristic positive carbon isotope excursion in carbonate and organic matter [*Scholle and Arthur*, 1980; *Pratt*, 1985; *Arthur et al.*, 1988], and a range of evidence suggests that this event produced a substantial decrease in atmospheric $p\mathrm{CO}_2$ [*Arthur et al.*, 1988; *Freeman and Hayes*, 1992; *Kuypers et al.*, 1999]. The OAE II interval also preserves trace element geochemical signatures suggestive of an increase in hydrothermally derived metals in some locations [*Orth et al.*, 1993; *Sinton and Duncan*, 1997; *Kerr*, 1998; *Larson and Erba*, 1999; *Snow et al.*, 2005], thus it provides an important case study to assess the biogeochemical role of iron in organic matter accumulation. Detailed geochemical, lithologic and sedimentologic investigations across the wide range of preserved C/T depositional settings provide the opportunity to rigorously assess the biogeochemical significance of iron in a global sense.

[31] One of the most thoroughly studied Cenomanian/Turonian stratigraphic intervals is the proposed stratotype section in the central Western Interior Basin (Bridge Creek Limestone Member: Colorado, United States [*Kennedy and Cobban*, 1991; *Kennedy et al.*, 2000]), which preserves a complete record of OAE II [*Pratt*, 1985; *Leckie*, 1985; *Elder*, 1989; *Dean and Arthur*, 1989; *Meyers et al.*, 2001; *Meyers and Sageman*, 2004]. The limestone-marlstone rhythms of the Bridge Creek Limestone record a Milankovitch orbital signature [*Sageman et al.*, 1997] from which a timescale has been derived [*Meyers et al.*, 2001; *Sageman et al.*, 2006], and the individual beds, traceable for 1000s of kilometers within the basin [*Hattin*, 1971; *Elder et al.*, 1994], provide a stratigraphic framework with detailed foraminiferal, nannofossil, ammonite and inoceramid biostratigraphy [e.g., *Leckie*, 1985; *Bralower*, 1988; *Elder*,
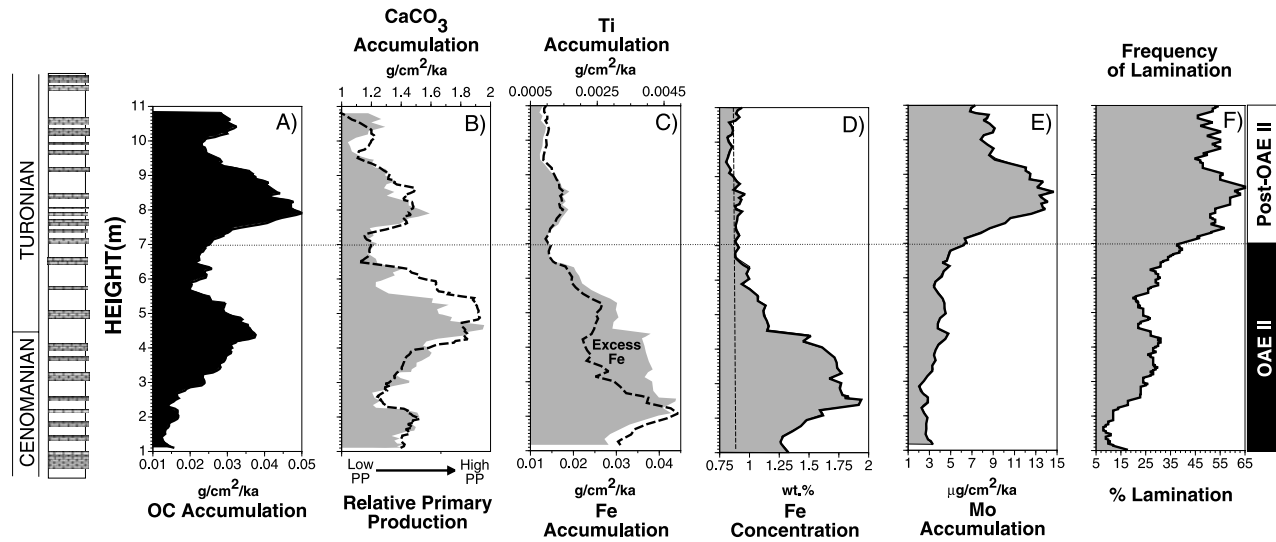
Figure 9. Data from the U.S.G.S. #1 Portland core [after *Meyers et al.*, 2001; *Meyers*, 2003; *Meyers et al.*, 2005]. (a) Organic carbon burial rates. (b) Relative primary production estimates based on carbonate accumulation rate (dashed line) and organic matter burial (shaded area) given a fabric-determined preservation index [see *Meyers et al.*, 2005]. (c) Fe accumulation (shaded area) and Ti accumulation (dashed line), a proxy for detrital mineral flux [*Meyers et al.*, 2001]. "Excess Fe" identifies an additional dissolved Fe source, decoupled from the local terrigenous flux. (d) Iron concentration data [*Meyers*, 2003]. (e) Molybdenum accumulation, an indicator of sulfide buildup in pore waters [*Zheng et al.*, 2000]. (f) Frequency of lamination, calculated by determining the number of laminated intervals (sampled every 2 cm) within a moving 2-m window. Frequency of lamination is based on the oxygen-related ichnocoenoses data of *Savrda* [1998]. All geochemical data represent 2-m moving averages (see *Meyers et al.* [2005] for discussion).

1989; *Kennedy and Cobban*, 1991]. Owing to this high-resolution chronostratigraphic framework, the Bridge Creek Limestone provides a remarkable opportunity to investigate OAE II expression in an epicontinental seaway environment. *Meyers et al.* [2001, 2005] conducted a detailed analysis of the controls on organic matter burial through this interval, including an assessment of the role of iron. A brief summary of their results is provided in Figure 9.

[32] Primary production estimates from the Bridge Creek Limestone are based on two independent methodologies (carbonate accumulation rate and an OC burial rate/preservation factor method, see *Meyers et al.* [2005] for a detailed discussion). These estimates indicate highest production during OAE II (Figure 9b), at a time of enhanced iron flux (Figure 9c). A large fraction of the iron ("Excess Fe" in Figure 9c) is decoupled from the local terrigenous flux (as measured by Ti accumulation; a proxy for detrital mineral flux [*Meyers et al.*, 2001]), consistent with a dissolved iron source during the event. Of particular importance to this study, the interval of elevated primary production and "Excess Fe" delivery during OAE II is also characterized by relatively modest organic carbon burial rates (Figure 9a). In contrast, the highest rates of organic carbon burial occur in the upper (post-OAE II) interval of reduced primary production, lower iron burial flux (no "Excess Fe"), and lower iron concentration.

[33] In the analysis of *Meyers et al.* [2001, 2005], molybdenum accumulation (MAR-Mo) was employed as a sensitive indicator of hydrogen sulfide buildup within pore

waters. The application of MAR-Mo in this capacity is founded upon laboratory and field-based studies that indicate the importance of molybdenum scavenging within sediment pore waters once a critical concentration of hydrogen sulfide ("switch point") is achieved [*Emerson and Huested*, 1991; *Crusius et al.*, 1996; *Helz et al.*, 1996; *Zheng et al.*, 2000; *Erickson and Helz*, 2000; *Vorlicek and Helz*, 2002]. It has also been proposed that changes in the size of the local or global molybdenum inventory may impact the magnitude of molybdenum accumulation [*Algeo*, 2004; *Algeo and Lyons*, 2006], in addition to factors such the availability of scavenging substrates (organic matter and pyrite [*Helz et al.*, 1996]). A comprehensive analysis of these potential controls on MAR-Mo is dependent upon a detailed understanding of the stratigraphy, sedimentology, paleobiology, and geochemistry of the deposits. Such an analysis is beyond the scope of the present study (many of these aspects are addressed by *Meyers et al.* [2005]), however, it will be demonstrated in the following discussion that the interpretation of MAR-Mo as a record of sulfide buildup within pore waters is consistent with numerous geologic data from the Bridge Creek Limestone.

[34] The OAE II interval at this location is characterized by low rates of molybdenum accumulation (Figure 9e), which is interpreted to be the consequence of low hydrogen sulfide concentration in sediment pore waters. This interval follows a major transgressive pulse [*Elder et al.*, 1994], during which the basin is transformed from a relatively restricted environment [*Sageman*, 1985] to one that shows

clear sedimentologic and paleobiologic indications of more oxygen-rich conditions, including the establishment of a prominent Tethyan fauna [*Kauffman*, 1984; *Elder and Kirkland*, 1985]. This transition is marked by a switch from the laminated organic-rich sediments of the Hartland Shale, exhibiting high molybdenum accumulation [*Sageman and Lyons*, 2004], to the more extensively bioturbated sediments of the lower Bridge Creek Limestone Member, exhibiting lower molybdenum accumulation (Figure 9e). These observations are inconsistent with the interpretation of MAR-Mo in terms of degree of basin restriction and deepwater renewal [see *Algeo and Lyons*, 2006]. MAR-Mo appears to dominantly reflect more localized changes in hydrogen sulfide buildup within sediments.

[35] A rapid increase in molybdenum accumulation follows OAE II (Figure 9e), coincident with the development of extensive sediment lamination (Figure 9f) [*Savrda*, 1998]. These observations support an interpretation of enhanced hydrogen sulfide concentration and reduced oxygen exposure time following OAE II. It is also feasible that a global reduction in the molybdenum inventory during OAE II accounts for some of the observed MAR-Mo variability in this record. However, this is likely a second-order effect due to two factors: (1) the major MAR-Mo shifts are extremely rapid relative to the residence time of molybdenum and (2) each MAR-Mo transition is associated with independent evidence for pronounced environmental changes.

[36] Taken together, the data in Figure 9 support the hypothesis that high iron flux during OAE II enhanced hydrogen sulfide buffering capacity at this site, yielding more effective bioturbation/bioirrigation and long oxygen exposure times. A reduction in iron supply following OAE II, attributable to a decreased detrital Fe flux and a diminished dissolved-Fe source, decreased buffering capacity and oxygen exposure time [*Meyers et al.*, 2005]. In addition to these factors, changes in labile organic matter concentration in the post-OAE II interval (e.g., due to sea level rise and decreased siliciclastic flux, see Ti accumulation in Figure 9c) must have played an important role in increasing hydrogen sulfide production [see *Meyers et al.*, 2005].

[37] The dissolved "Excess Fe" delivery observed during OAE II has several possible sources. As mentioned previously, such iron could be derived from a diagenetically remobilized iron source from elsewhere in the seaway/global ocean, or may be the consequence of enhanced hydrothermal iron delivery [*Sinton and Duncan*, 1997; *Larson and Erba*, 1999; *Leckie et al.*, 2002; *Erba*, 2004; *Snow et al.*, 2005]. If sedimentary iron enrichment via diagenetic remobilization requires an anoxic sulfidic water mass, as suggested by many authors [*Raiswell and Canfield*, 1998; *Anderson and Raiswell*, 2004; *Lyons and Severmann*, 2006], it seems an unlikely candidate for the observed "Excess Fe" record. As noted above, independent geochemical, faunal, and sedimentologic characteristics of these sediments are inconsistent with a persistent sulfidic water mass during OAE II. In fact, more sulfidic conditions occur following the OAE II (Figures 9e and 9f), during a time of reduced dissolved iron flux (Figure 9c). Coastal ocean model experiments [*Kump and Slingerland*, 1999] further demonstrate that turbulent mixing in the Western

Interior Seaway would have rapidly eliminated water column stratification.

[38] With respect to a hydrothermal source, the OAE II interval contains trace metal enrichments that have been previously interpreted as reflecting a hydrothermal signal, presumably derived from the Caribbean LIP (Large Igneous Province) that was forming just south of the Western Interior Seaway at this time [*Orth et al.*, 1993; *Snow et al.*, 2005]. These trace metal enrichments are most pronounced in the southern Western Interior Seaway, and decrease in magnitude toward the northern portion of seaway [*Orth et al.*, 1993]. The onset of "Excess Fe" accumulation in the Bridge Creek Limestone Member (Figure 9) is coincident with a hypothesized ingress of Tethyan oxygen minimum zone waters into the basin, because of the achievement of sea level rise sufficient to overcome the silled southern aperture of the Western Interior Seaway [*Arthur et al.*, 1998; *Arthur and Sageman*, 2004]. Given the proximal location of the Caribbean LIP, it is plausible that the suboxic to anoxic water of the Tethyan oxygen minimum zone facilitated transport of reduced hydrothermal iron into the Western Interior Seaway.

[39] In summary, the data in Figure 9 demonstrate an increase in primary production associated with enhanced iron delivery during the "oceanic anoxic event," but also relatively oxic depositional conditions leading to lower organic carbon burial. The proximity of this site to a Tethyan hydrothermal iron source appears to account for greater sulfide buffering capacity, and thus more thoroughly bioturbated sediments. Although the observed history of OAE II at this location is unique in some regards [see *Tsikos et al.*, 2004], these results underscore the potential for a complex role of iron in organic matter burial during the event. Such complexities may partially explain the observed diachroneity of OAE II organic carbon enrichment at different locations globally [e.g., *Tsikos et al.*, 2004], as well as variability in the magnitude of organic carbon burial. This should be expected if some environments are more sensitive to iron-forced production, while others are more prone to iron-forced preservational changes. The complete answer to this question awaits detailed geochemical burial flux analyses across the broad spectrum of preserved C/T depositional environments.

5. Conclusions

[40] Although iron is recognized as an important control on organic matter production in the modern ocean, and the role of iron in early diagenesis is well established, little attention has been given to the relative impact of these processes on organic matter burial. The results of this study indicate that enhanced organic matter delivery to the sediment due to iron fertilization can potentially be compensated for by an increase in dissolved sulfide buffering within sediments, which yields an increase in bioturbation/bioirrigation and oxygen exposure time. The biogeochemical linkage between marine iron and phosphorous cycles provides a positive feedback, whereby enhanced iron oxide content in the sediment serves as a trap for remineralized phosphorous, decreasing the flux of this

nutrient to the water column, and potentially diminishing primary production. The combination of these mechanisms is designated the "sulfide buffer/phosphorous trap hypothesis."

[41] The intricate processes addressed in this study have been investigated using numerical models that are tied strongly to geochemical data from ancient and modern sediments. Biogeochemical model experiments highlight the dependence of pore water sulfide levels on the concentration of labile organic matter relative to the concentration of reactive iron. These experiments also indicate that marine settings with low sediment burial rates should be most sensitive to the sulfide buffering mechanism, since these environments are characterized by relatively low hydrogen sulfide production rates [*Toth and Lerman*, 1977; *Canfield*, 1989b], and minor changes in the thickness of the zone of bioturbation can represent hundreds to thousands of years of degradation. Such sediment burial rates are typical of ancient source rocks [*Ibach*, 1982].

[42] Importantly, the "sulfide buffer/phosphorous trap hypothesis" provides an alternative mechanism for organic matter burial throughout Earth history, one that does not require initial changes in primary production [*Pedersen and Calvert*, 1990] or the development of stratified euxinic environments [*Demaison and Moore*, 1980]. This biogeochemical mechanism is particularly relevant to the development of "transgressive source rocks," where shoaling of the SRZ within sediments is a natural consequence of biogeochemical changes associated with siliciclastic sediment starvation (e.g., sediment trapping in estuaries) during sea level rise. Such conditions can promote increased hydrogen sulfide production (high concentrations of labile organic matter) and decreased hydrogen sulfide removal (lower reactive iron concentration).

[43] Changes in pelagic and hemipelagic biomineralization during the Phanerozoic, such as the widespread deposition of chalk and marl during the Cretaceous, may have played an important role in setting the stage for organic carbon burial events by decreasing terrigenous reactive iron concentration. Examination of the OAE II interval in the Bridge Creek Limestone Member demonstrates the potential for a complex role of iron in organic matter accumulation. Geochemical burial flux data indicate that the diagenetic controls on organic matter burial dominate, largely overprinting the observed changes in primary production. Taken together, the model experiments and geochemical data suggest that changes in iron delivery can serve as a principal control on production, preservation and marine organic matter burial.

Appendix A: Parameters and Equations Utilized in the Models Displayed in Figures 4 and 5

[44] The equations utilized in the models displayed in Figures 4 and 5 are as follows:

$$\rho = G\alpha\rho_{OM} + (1 - G\alpha) * \rho_{Diluent} \qquad (A1)$$

$$\omega = \frac{R_{burial}}{\rho(1-\phi)} \qquad (A2)$$

Table A1. Appendix A Variables

Variable	Definition	Unit of Measure
G	organic carbon reaching sediment sulfate reduction zone	wt %
C_{Fe}	reactive iron	wt %
C_{H2S}	initial pore water hydrogen sulfide concentration	mol L^{-1}
dG/dt	rate of organic matter decomposition	wt % OC a^{-1}
k_{org}	first-order rate constant for sulfate reduction [*Toth and Lerman*, 1977; *Westrich and Berner*, 1984]	1 a^{-1}
k_{Fe}	H$_2$S dependent rate constant for iron sulfidization [*Poulton et al.*, 2004]	L$^{0.5}$ mol$^{-0.5}$ a^{-1}
k^*_{Fe}	H$_2$S independent rate constant for iron sulfidization [*Raiswell and Canfield*, 1996]	1 a^{-1}
dH_2S/dt	hydrogen sulfide production or removal rate	mol H$_2$S cm^{-3} a^{-1}
R$_{burial}$	sediment burial rate	10^{-4} to 10^2 g cm^{-2} a^{-1}
t	time	a
α	stoichiometric factor relating organic matter to organic carbon, 2.5	
ρ	mean density of total sediment solids	g cm^{-3}
ρ_{OM}	organic matter particle density	1 g cm^{-3}
$\rho_{Diluent}$	diluent particle density	g cm^{-3}
φ	sediment porosity, 0.8	
$\rho(1 - \varphi)$	dry bulk density	g cm^{-3}
ω	sedimentation rate at sediment-water interface	cm a^{-1}

Equations pertaining to sulfide production are the following:

$$k_{org} = 0.057\omega^{1.94} \qquad (A3)$$

$$\frac{dH_2S}{dt} = k_{org}G\left(\frac{\rho(1-\phi)}{\phi}\right)\left(\frac{0.5}{12.01 \text{ gC/mol}}\right) \qquad (A4)$$

Equations pertaining to sulfide removal are the following:

$$\text{lepidocrocite } k_{Fe}1.8 \times 10^4 \text{ L}^{0.5}\text{mol}^{-0.5}\text{a}^{-1} \qquad (A5)$$

$$\text{magnatite } k_{Fe} = 1.7 \times 10^2 \text{ L}^{0.5}\text{mol}^{-0.5}\text{a}^{-1} \qquad (A6)$$

$$\text{goethite } k_{Fe} = 1.3 \times 10^2 \text{ L}^{0.5}\text{mol}^{-0.5}\text{a}^{-1} \qquad (A7)$$

$$\text{hematite } k_{Fe} = 4.7 \times 10^1 \text{ L}^{0.5}\text{mol}^{-0.5}\text{a}^{-1} \qquad (A8)$$

$$\text{poorly reactive iron } k_{Fe}^{*} = 2.9 \times 10^{-7}\text{a}^{-1} \qquad (A9)$$

$$\frac{dH_2S}{dt} = -k_{Fe}C_{Fe}\left(\frac{\rho(1-\phi)}{\phi}\right)\left(\frac{1}{55.85 \text{ gFe/mol}}\right)(C_{H_2S})^{0.5}$$

$$(A10)$$

See Table A1 for a list of variables and definitions.

[45] Although not directly apparent from equation (A10), wt % OC (G) influences the calculated sulfide removal rates. Owing to the low density of organic matter ($\sim$1 g cm^{-3}), the sulfide removal rate is minimized when wt % OC concentration is maximized because this results in a low bulk density (equation (A10)). The estimates provided in Figures 4 and 5 are conservative (low) sulfide removal rates, calculated using 36 wt % OC (or 90 wt % CH$_2$O) and 2 wt % Fe. Calculations using 1 wt % OC and 10 wt % OC increase sulfide removal rates by a factor of $\sim$2.2 and $\sim$1.9, respectively, because of increased bulk density. Given the large (orders of magnitude) range of reactivity associated with the minerals investigated in Figure 4, this variability is not substantial.

[46] The diluent particle density ($\rho_{Diluent}$) for the sulfide removal estimates is determined using the appropriate particle density and stoichiometry for each iron-bearing mineral phase (e.g., hematite, magnetite, etc.), and a background diluent particle density of 2.65 g cm^{-3}, which is intermediate between the density of calcite and silicate minerals. This background diluent contains no iron. The sulfide removal rate for "poorly reactive iron" is calculated using the density and stoichiometry of ilmenite.

[47] Sulfide production rates are calculated using a diluent particle density ($\rho_{Diluent}$) of 2.65 g cm^{-3}. A sedimentation rate dependent rate constant for sulfide production (equation (A4)) is used [*Toth and Lerman*, 1977], with a maximum value based on the decomposition of fresh plankton (24 a^{-1} [*Westrich and Berner*, 1984]).

Appendix B: Pore Water Sulfide Model Utilized in Figure 6

[48] The pore water sulfide model used to investigate linkages between reactive iron burial, sulfide buffering and oxygen exposure time in marine sediments is adapted from *Raiswell and Canfield*'s [1996] analysis of Peru Margin sediments.

$$\rho_s = G\alpha\rho_{OM} + (1 - G\alpha) * \rho_{Diluent} \qquad (B1)$$

Table B1. Appendix B Variables

Variable	Definition	Unit of Measure
	Input	
x	depth	0–100 cm
ω	sedimentation rate at sediment-water interface	0.005 cm a^{-1}
ρ_{OM}	organic matter density	1 g cm^{-3}
$\rho_{Diluent}$	diluent density	2.65 g cm^{-3}
φ	sediment porosity	0.8
α_G	stoichiometric factor for organic carbon	mol (12.01 g)$^{-1}$
α_{Fe}	stoichiometric factor for iron	mol (55.85 g)$^{-1}$
G_o	initial organic carbon at the sediment-water interface	5 wt %
$C_{Fe,o}$	initial reactive iron at the sediment-water interface	0.5–10 wt %
k_{org}	first-order rate constant for sulfate reduction	5 $\times$ 10^{-6} a^{-1}
k_{Fe}	first-order rate constant for iron sulfidization	2.9 $\times$ 10^{-7} a^{-1}
D_s	diffusion coefficient for sulfide	265 cm^2 a^{-1}
	Output	
ρ_s	calculated density of total solids	g cm^{-3}
C_s	calculated pore water sulfide concentration	mM

$$C_s(x) = A - \left(\frac{0.5 \, k_{org}G_o e^{(-k_{org}x/\omega)}\alpha_G\rho_s(1-\phi)/\phi}{D_s(k_{org}/\omega)^2 + k_{org}}\right) + \left(\frac{2 \, k_{Fe}C_{Fe,o}e^{(-k_{Fe}x/\omega)}\alpha_{Fe}\rho_s(1-\phi)/\phi}{D_s(k_{Fe}/\omega)^2 + k_{Fe}}\right)$$

$$(B2)$$

$$A = \left(\frac{0.5 \, k_{org}G_o(1-\phi)/\phi}{D_s(k_{org}/\omega)^2 + k_{org}}\right) - \left(\frac{2 \, k_{Fe}C_{Fe,o}(1-\phi)/\phi}{D_s(k_{Fe}/\omega)^2 + k_{Fe}}\right)$$

$$(B3)$$

See Table B1 for a list of variables and definitions.

References

Adam, P., J. C. Schmid, B. Mycke, C. Strazielle, J. Connan, A. Huc, A. Riva, and P. Albrecht (1993), Structural investigation of nonpolar sulfur cross-linked macromolecules in petroleum, *Geochim. Cosmochim. Acta*, 57, 3395–3419.

Algeo, T. J. (2004), Can marine anoxic events draw down the trace-element inventory of sea water?, *Geology*, 32, 1057–1060.

Algeo, T. J., and T. W. Lyons (2006), Mo–total organic carbon covariation in modern anoxic marine environments: Implications for analysis of paleoredox and paleohydrographic conditions, *Paleoceanography*, 21, PA1016, doi:10.1029/2004PA001112.

Aller, R. C. (1990), Bioturbation and manganese cycling in hemipelagic sediments, *Philos. Trans. R. Soc. London, Ser. A*, 331, 51–68.

Anderson, T. F., and R. Raiswell (2004), Sources and mechanisms for the enrichment of highly reactive iron in euxinic Black Sea sediments, *Am. J. Sci.*, 304, 203–233.

Arthur, M. A., and B. B. Sageman (1994), Marine black shales: A review of depositional mechanisms and environments of ancient deposits, *Annu. Rev. Earth Planet. Sci.*, 22, 499–552.

Arthur, M. A., and B. B. Sageman (2004), Sea level control on source rock development: Perspectives from the Holocene Black Sea, the mid-Cretaceous western interior Basin of North America, and the Late Devonian Appalachian Basin, in *The Deposition of Organic Carbon-Rich Sediments: Models, Mechanisms and Consequences*, edited by N. B. Harris and B. Pradier, pp. 35–59, Soc. For Sediment. Geol., Tulsa, Okla.

Arthur, M. A., W. E. Dean, and S. O. Schlanger (1985), Variations in the global carbon cycle during the Cretaceous related to climate, volcanism, and changes in atmospheric CO_2, in *The Carbon Cycle and Atmospheric CO_2: Natural Variations Archean to Present*, *Geophys. Monogr. Ser.*, vol. 32, edited by E. T. Sundquist and W. S. Broecker, pp. 504–529, AGU, Washington, D. C.

Arthur, M. A., W. E. Dean, and L. M. Pratt (1988), Geochemical and climatic effects of increased marine organic carbon burial at the Cenomanian/Turonian boundary, *Nature*, *335*, 714–717.

Arthur, M. A., B. B. Sageman, W. E. Dean, R. L. Slingerland, L. R. Kump, and T. S. White (1998), Transgression, advection of oxygen-depleted water, and eutrophication of the mid-Cretaceous Western Interior Seaway of North America, paper presented at Annual Meeting, Geol. Soc. of Am., Toronto, Ont. Canada, 26–29 Oct.

Behrenfeld, M. J., and Z. S. Kolber (1999), Widespread iron limitation of phytoplankton in the South Pacific Ocean, *Science*, *283*, 840–843.

Behrenfeld, M. J., A. J. Bale, Z. S. Kolber, J. Aiken, and P. G. Falkowski (1996), Confirmation of iron limitation of phytoplankton photosynthesis in the equatorial Pacific Ocean, *Nature*, *383*, 508–511.

Berner, R. A. (1980), *Early Diagenesis: A Theoretical Approach*, 256 pp, Princeton Univ. Press, Princeton, N. J.

Berner, R. A. (1985), Sulfate reduction, organic matter decomposition and pyrite formation, *Philos. Trans. R. Soc. London, Ser. A*, *315*, 25–38.

Boyd, P. W., et al. (2000), A mesoscale phytoplankton bloom in the polar Southern Ocean stimulated by iron fertilization, *Nature*, *407*, 695–702.

Boyle, E. A., B. A. Bergquist, R. A. Kayser, and N. Mahowald (2005), Iron, manganese, and lead at Hawaii Ocean Time-series station ALOHA: Temporal variability and an intermediate water hydrothermal plume, *Geochim. Cosmochim. Acta*, *69*, 933–952.

Bralower, T. J. (1988), Calcareous nannofossil biostratigraphy and assemblages of the Cenomanian-Turonian boundary interval: Implications for the origin and timing of oceanic anoxia, *Paleoceanography*, *3*, 275–316.

Canfield, D. E. (1989a), Reactive iron in marine sediments, *Geochim. Cosmochim. Acta*, *53*, 619–632.

Canfield, D. E. (1989b), Sulfate reduction and oxic respiration in marine sediments: Implications for organic carbon preservation in euxinic sediments, *Deep Sea Res., Part A*, *36*, 121–138.

Canfield, D. E., R. Raiswell, and S. Bottrell (1992), The reactivity of sedimentary iron minerals toward sulfide, *Am. J. Sci.*, *292*, 659–683.

Canfield, D. E., T. W. Lyons, and R. Raiswell (1996), A model for iron deposition to euxinic Black Sea sediments, *Am. J. Sci.*, *296*, 818–834.

Cha, H. J., C. B. Lee, B. S. Kim, M. S. Choi, and K. C. Ruttenberg (2005), Early diagenetic redistribution and burial of phosphorous in the sediments of the southwestern East Sea (Japan Sea), *Mar. Geol.*, *216*, 127–143.

Chanton, J. P., C. S. Martens, and M. B. Goldhaber (1987), Biogeochemical cycling in an organic-rich coastal marine basin. 7. Sulfur mass balance, oxygen uptake and sulfide retention, *Geochim. Cosmochim. Acta*, *51*, 1187–1199.

Chase, Z., K. S. Johnson, V. A. Elrod, J. N. Plant, S. E. Fitzwater, L. Pickell, and C. M. Sakamoto (2005), Manganese and iron distributions off central California influenced by upwelling and shelf width, *Mar. Chem.*, *95*, 235–254.

Crusius, J., S. Calvert, T. Pedersen, and D. Sage (1996), Rhenium and molybdenum enrichments in sediments as indicators of oxic, suboxic, and sulfidic conditions of deposition, *Earth Planet. Sci. Lett.*, *145*, 65–78.

Dean, W. E., and M. A. Arthur (1989), Iron-sulfur-carbon relationships in organic-carbon rich sequences I: Cretaceous Western Interior Seaway, *Am. J. Sci.*, *289*, 708–743.

Demaison, G. J., and G. T. Moore (1980), Anoxic environments and oil source bed genesis, *AAPG Bull.*, *64*, 1179–1209.

Elder, W. P. (1989), Molluscan extinction patterns across the Cenomanian-Turonian stage boundary in the western interior of the United States, *Paleobiology*, *15*, 299–320.

Elder, W. P., and J. I. Kirkland (1985), Stratigraphy and depositional environments of the Bridge Creek Limestone Member of the Greenhorn Limestone at Rock Canyon Anticline near Pueblo, Colorado, in *Fine-Grained Deposits and Biofacies of the Cretaceous Western Interior Seaway: Evidence of Cyclic Sedimentary Processes*, edited by L. M. Pratt et al., pp. 122–134, Soc. for Sediment. Geol., Tulsa, Okla.

Elder, W. P., E. R. Gustason, and B. B. Sageman (1994), Basinwide correlation of parasequences in the Greenhorn cyclothem, western interior, U.S., *Geol. Soc. Am. Bull.*, *106*, 892–902.

Emerson, S. R., and S. S. Huested (1991), Ocean anoxia and the concentrations of molybdenum and vanadium in seawater, *Mar. Chem.*, *34*, 177–196.

Erba, E. (2004), Calcareous nannofossils and Mesozoic oceanic anoxic events, *Mar. Micropaleontol.*, *52*, 85–106.

Erickson, B. E., and G. R. Helz (2000), Molybdenum (VI) speciation in sulfidic waters: Stability and lability of thiomolybdates, *Geochim. Cosmochim. Acta*, *64*, 1149–1158.

Falkowski, P. G. (1997), Evolution of the nitrogen cycle and its influence on the biological sequestration of CO_2 in the ocean, *Nature*, *387*, 272–275.

Falkowski, P. G., R. T. Barber, and V. Smetacek (1998), Biogeochemical controls and feedbacks on ocean primary production, *Science*, *281*, 200–206.

Firme, G. F., E. L. Rue, D. A. Weeks, K. W. Bruland, and D. A. Hutchins (2003), Spatial and temporal variability in phytoplankton iron limitation along the California coast and consequences for Si, N, and C biogeochemistry, *Global Biogeochem. Cycles*, *17*(1), 1016, doi:10.1029/2001GB001824.

Freeman, K. H., and J. M. Hayes (1992), Fractionation of carbon isotopes by phytoplankton and estimates of ancient CO2 levels, *Global Biogeochem. Cycles*, *6*(2), 185–198.

Froelich, P. N., G. P. Klinkhammer, M. L. Bender, N. A. Luedtke, G. R. Heath, D. Cullen, P. Dauphin, D. Hammond, B. Hartman, and V. Maynard (1979), Early oxidation of organic matter in pelagic sediments of the eastern equatorial Atlantic: Suboxic diagenesis, *Geochim. Cosmochim. Acta*, *43*, 1075–1090.

Haq, B. U., J. Hardenbol, and P. R. Vail (1987), Chronology of fluctuating sea levels since the Triassic, *Science*, *235*, 1156–1167.

Hartnett, H. E., R. G. Keil, J. I. Hedges, and A. H. Devol (1998), Influence of oxygen exposure time on organic carbon preservation in continental margin sediments, *Nature*, *391*, 572–574.

Hattin, D. E. (1971), Widespread, synchronously deposited, burrow-mottled limestone beds in Greenhorn Limestone (Upper Cretaceous) of Kansas and central Colorado, *Am. Assoc. Pet. Geol. Bull.*, *55*, 412–431.

Hebting, Y., P. Schaeffer, A. Behrens, P. Adam, G. Schmitt, P. Schneckenburger, S. M. Bernasconi, and P. Albrecht (2006), Biomarker evidence for a major preservation pathway of sedimentary organic carbon, *Science*, *312*, 1627–1631.

Hedges, J. I., and R. G. Keil (1995), Sedimentary organic matter preservation: An assessment and speculative synthesis, *Mar. Chem.*, *49*, 81–115.

Helz, G. R., C. V. Miller, J. M. Charnock, J. F. W. Mosselmans, R. A. D. Pattrick, C. D. Garner, and D. J. Vaughan (1996), Mechanisms of molybdenum removal from the sea and its concentration in black shales: EXAFS evidence, *Geochim. Cosmochim. Acta*, *60*, 3631–3642.

Huber, B. T., D. A. Hodell, and C. P. Hamilton (1995), Middle-Late Cretaceous climate of the southern high latitudes: Stable isotopic evidence for minimal equator-to-pole thermal gradients, *GSA Bull.*, *107*, 1164–1191.

Hutchins, D. A., and K. W. Bruland (1998), Iron-limited diatom growth and Si:N uptake ratios in coastal upwelling regime, *Nature*, *393*, 561–564.

Hutchins, D. A., G. R. DiTullio, Y. Zhang, and K. W. Bruland (1998), An iron limitation mosaic in the California upwelling regime, *Limnol. Oceanogr.*, *43*, 1037–1054.

Ibach, L. E. J. (1982), Relationship between sedimentation rate and total organic carbon content in ancient marine sediments, *AAPG Bull.*, *66*, 170–188.

Ingall, E., R. M. Bustin, and P. Van Cappellen (1993), Influence of water column anoxia on the burial and preservation of carbon and phosphorous in marine shales, *Geochim. Cosmochim. Acta*, *57*, 303–316.

Jenkyns, H. C. (1980), Cretaceous anoxic events: From continents to oceans, *J. Geol. Soc. London*, *137*, 171–188.

Jenkyns, H. C., A. Forster, S. Schouten, and J. S. Sinninghe Damsté (2004), High temperatures in the Late Cretaceous Arctic Ocean, *Nature*, *432*, 888–892.

Jickells, T. D., and L. J. Spokes (2001), Atmospheric iron inputs to the oceans, in *The Biogeochemistry of Iron in Seawater*, edited by D. R. Turner and K. Hunter, pp. 85–121, John Wiley, New York.

Jones, C. E., and H. C. Jenkyns (2001), Seawater strontium isotopes, oceanic anoxic events, and seafloor hydrothermal activity in the Jurassic and Cretaceous, *Am. J. Sci.*, *301*, 112–149.

Jorgensen, B. B. (1977), The sulfur cycle of a coastal marine sediment (Limfjorden, Denmark), *Limnol. Oceanogr.*, *22*, 814–832.

Junium, C. K., A. L. Zerkle, and M. A. Arthur (2006), The fix is on! Nitrogen isotope

evidence for high surface-water iron availability during oceanic anoxic event II, *Eos Trans. AGU*, *87*, Fall Meet. Suppl., Abstract PP31D-05.

Kauffman, E. G. (1984), Paleobiogeography and evolutionary response dynamic in the Cretaceous Western Interior Seaway of North America, in *Jurassic-Cretaceous Biochronology and Paleogeography of North America*, edited by G. E. G. Westermann, pp. 273–306, Geol. Assoc. of Canada, St. John's, Nfld., Canada.

Kennedy, W. J., and W. A. Cobban (1991), Stratigraphy and interregional correlation of the Cenomanian-Turonian transition in the western interior of the United States near Pueblo, Colorado, a potential boundary stratotype for the base of the Turonian stage, *Newsl. Stratigr.*, *24*(1/2), 1–33.

Kennedy, W. J., I. Walaszczyk, and W. A. Cobban (2000), Pueblo, Colorado, USA, candidate Global Boundary Stratotype Section and point for the base of the Turonian stage of the Cretaceous, and for the base of the middle Turonian substage, with a revision on the Inoceramidae (Bivalvia), *Acta Geol. Pol.*, *50*, 295–334.

Kerr, A. C. (1998), Oceanic plateau formation: A cause of mass extinctions and black shale deposition around the Cenomanian-Turonian boundary?, *J. Geol. Soc. London*, *155*, 619–626.

Kolber, Z. S., R. T. Barber, K. H. Coale, S. E. Fitzwateri, R. M. Greene, K. S. Johnson, S. Lindley, and P. G. Falkowski (1994), Iron limitation of phytoplankton photosynthesis in the equatorial Pacific ocean, *Nature*, *371*, 145–149.

Krom, M. D., and R. A. Berner (1980), Adsorption of phosphate in anoxic marine sediments, *Limnol. Oceanogr.*, *25*, 797–806.

Kumar, N., R. F. Anderson, R. A. Mortlock, P. N. Froelich, P. Kubik, B. Dittrich-Hannen, and M. Suter (1995), Increased biological productivity and export production in the glacial Southern Ocean, *Nature*, *378*, 675–680.

Kump, L. R., and R. L. Slingerland (1999), Circulation and stratification of the early Turonian Western Interior Seaway: Sensitivity to a variety of forcings, in *The Evolution of the Cretaceous Ocean-Climatic System*, edited by E. Barrera and C. C. Johnson, pp. 181–190, Geol. Soc. of Am., Boulder, Colo.

Kuypers, M. M., R. D. Pancost, and J. S. Sinninghe Damsté (1999), A large and abrupt fall in atmospheric CO_2 concentrations during Cretaceous times, *Nature*, *399*, 342–345.

Kuypers, M. M., Y. van Breugel, S. Schouten, E. Erba, and J. S. Sinninghe Damsté (2004), N_2-fixing cyanobacteria supplied nutrient N for Cretaceous oceanic anoxic events, *Geology*, *32*, 853–856.

Larson, R. L., and E. Erba (1999), Onset of the mid-Cretaceous greenhouse in the Barremian-Aptian: Igneous events and the biological, sedimentary, and geochemical responses, *Paleoceanography*, *14*, 663–678.

Leckie, R. M. (1985), Foraminifera of the Cenomanian-Turonian boundary interval, Greenhorn Formation, Rock Canyon Anticline, Pueblo, Colorado, in *Fine-Grained Deposits and Biofacies of the Cretaceous Western Interior Seaway: Evidence of Cyclic Sedimentary Processes*, edited by L. M. Pratt et al., pp. 139–149, Soc. for Sediment. Geol., Tulsa, Okla.

Leckie, R. M., T. J. Bralower, and R. Cashman (2002), Oceanic anoxic events and plankton evolution: Biotic response to tectonic forcing during the mid-Cretaceous, *Paleoceanography*, *17*(3), 1041, doi:10.1029/2001PA000623.

Lyons, T. W. (1997), Sulfur isotopic trends and pathways of iron sulfide formation in upper Holocene sediments of the anoxic Black Sea, *Geochim. Cosmochim. Acta*, *61*, 3367–3382.

Lyons, T. W., and S. Severmann (2006), A critical look at iron paleoredox proxies: New insights from modern euxinic marine basins, *Geochem. Cosmochim. Acta*, *70*, 5698–5722.

Martin, J. H. (1990), Glacial-interglacial CO_2 change: The iron hypothesis, *Paleoceanography*, *5*, 1–13.

Martin, J. H., and S. E. Fitzwater (1988), Iron deficiency limits phytoplankton growth in the north-east Pacific subarctic, *Nature*, *331*, 341–343.

Martin, J. H., R. M. Gordon, S. Fitzwater, and W. W. Broenkow (1989), VERTEX: Phytoplankton/iron studies in the Gulf of Alaska, *Deep Sea Res., Part A*, *36*, 649–680.

Martin, J. H., et al. (1994), Testing the iron hypothesis in ecosystems of the equatorial Pacific Ocean, *Nature*, *371*, 123–129.

Meyers, P. A. (2006), Paleoceanographic and paleoclimatic similarities between Mediterranean sapropels and Cretaceous black shales, *Palaeogeorg. Palaeoclimatol. Palaeoecol.*, *235*, 305–320.

Meyers, S. R. (2003), Integrated cyclostratigraphy and biogeochemistry of the Cenomanian/Turonian boundary interval, Western Interior Basin, North America, 393 pp., Ph.D. thesis, Northwestern Univ., Evanston, Ill.

Meyers, S. R., and B. B. Sageman (2004), Detection, quantification, and significance of hiatuses in pelagic and hemipelagic strata, *Earth Planet. Sci. Lett.*, *224*, 55–72.

Meyers, S. R., B. B. Sageman, and L. A. Hinnov (2001), Integrated quantitative stratigraphy of the Cenomanian-Turonian Bridge Creek Limestone Member using evolutive harmonic analysis and stratigraphic modeling, *J. Sediment. Res.*, *71*, 627–643.

Meyers, S. R., B. B. Sageman, and T. W. Lyons (2005), Organic carbon burial rate and the molybdenum proxy: Theoretical framework and application to Cenomanian-Turonian oceanic anoxic event 2, *Paleoceanography*, *20*, PA2002, doi:10.1029/2004PA001068.

Michaels, A. F., D. Olson, J. L. Sarmiento, J. W. Ammerman, K. Fanning, R. Jahnke, A. H. Knap, F. Lipschultz, and J. M. Prospero (1996), Inputs, losses and transformations of nitrogen and phosphorus in the pelagic North Atlantic Ocean, *Biogeochemistry*, *35*, 181–226.

Murphy, A. E., B. B. Sageman, D. J. Hollander, T. W. Lyons, and C. E. Brett (2000), Black shale deposition and faunal overturn in the Devonian Appalachian basin: Clastic starvation, seasonal water-column mixing, and efficient biolimiting nutrient recycling, *Paleoceanography*, *15*, 280–291.

Orth, C. J., M. Attrep, L. R. Quintana, W. P. Elder, E. G. Kauffman, R. Diner, and T. Villautol (1993), Elemental abundance anomalies in the late Cenomanian extinction interval: A search for the source(s), *Earth Planet. Sci. Lett.*, *117*, 189–204.

Pedersen, T. F., and S. E. Calvert (1990), Anoxia vs. productivity: What controls the formation of organic-carbon-rich sediments and sedimentary rocks?, *AAPG Bull.*, *74*, 454–466.

Poulton, S. W., and D. E. Canfield (2005), Development of a sequential extraction procedure for iron: Implications for iron partitioning in continentally derived particulates, *Chem. Geol.*, *214*, 209–221.

Poulton, S. W., and R. Raiswell (2002), The low-temperature geochemical cycle of iron: From continental fluxes to marine sediment deposition, *Am. J. Sci.*, *302*, 774–805.

Poulton, S. W., M. D. Krom, and R. Raiswell (2004), A revised scheme for the reactivity of iron (oxyhydr)oxide minerals towards dissolved sulfide, *Geochim. Cosmochim. Acta*, *18*, 3703–3715.

Pratt, L. M. (1985), Isotopic studies of organic matter and carbonate in rocks of the Greenhorn marine cycle, in *Fine-Grained Deposits and Biofacies of the Cretaceous Western Interior Seaway: Evidence of Cyclic Sedimentary Processes*, edited by L. M. Pratt et al., pp. 38–48, Soc. for Sediment. Geol., Tulsa, Okla.

Premoli Silva, I., and W. V. Sliter (1999), Cretaceous paleoceanography: Evidence from planktonic foraminiferal evolution, in *The Evolution of the Cretaceous Ocean-Climatic System*, edited by E. Barrera and C. C. Johnson, pp. 301–328, Geol. Soc. of Am., Boulder, Colo.

Raiswell, R. (2006), Towards a global highly reactive iron cycle, *J. Geochem. Explor.*, *88*, 436–439.

Raiswell, R., and H. J. Al-Biatty (1989), Depositional and diagenetic C-S-Fe signatures in early Paleozoic normal marine shales, *Geochim. Cosmochim. Acta*, *53*, 1147–1152.

Raiswell, R., and D. E. Canfield (1996), Rates of reaction between silicate iron and dissolved sulfide in Peru Margin sediments, *Geochim. Cosmochim. Acta*, *60*, 2777–2787.

Raiswell, R., and D. E. Canfield (1998), Sources of iron for pyrite formation in marine sediments, *Am. J. Sci.*, *298*, 219–245.

Ruttenberg, K. C. (2003), The global phosphorous cycle, in *Treatise on Geochemistry*, vol. 8, edited by W. H. Schlesinger, pp. 585–643, Elsevier, New York.

Sageman, B. B. (1985), High-resolution stratigraphy and paleobiology of the Hartland Shale Member: Analysis of an oxygen-deficient epicontinental sea, in *Fine-Grained Deposits and Biofacies of the Cretaceous Western Interior Seaway: Evidence of Cyclic Sedimentary Processes*, edited by L. M. Pratt et al., pp. 112–121, Soc. for Sediment. Geol., Tulsa, Okla.

Sageman, B. B. (1989), The benthic boundary biofacies model: Hartland Shale Member, Greenhorn Formation (Cenomanian), western interior, North America, *Palaeogeogr. Palaeoclimatol. Palaeoecol.*, *74*, 87–110.

Sageman, B. B., and T. Lyons (2004), Geochemistry of fine-grained sediments and sedimentary rocks, in *Treatise on Geochemistry*, vol. 7, edited by F. MacKenzie, pp. 115–158, Elsevier, New York.

Sageman, B. B., J. Rich, M. A. Arthur, G. E. Birchfield, and W. E. Dean (1997), Evidence For Milankovitch periodicities in Cenomanian-Turonian lithologic and geochemical cycles, western interior U.S., *J. Sediment. Res.*, *67*, 286–301.

Sageman, B. B., A. E. Murphy, J. P. Werne, C. A. Ver Straeten, D. J. Hollander, and T. W. Lyons (2003), A tale of shales: The relative roles of production, decomposition, and dilution in the accumulation of organic-rich strata, Middle-Upper Devonian, Appalachian basin, *Chem. Geol.*, *195*, 229–273.

Sageman, B. B., S. R. Meyers, and M. A. Arthur (2006), Orbital time scale and new C-isotope record for Cenomanian-Turonian boundary stratotype, *Geology*, *34*, 125–128.

Saltzman, M. R. (2005), Phosphorous, nitrogen, and the redox evolution of the Paleozoic oceans, *Geology*, *33*, 573–576.

Savrda, C. E. (1998), Ichnology of the Bridge Creek Limestone: Evidence for temporal and spatial variations in paleo-oxygenation in the Western Interior Seaway, in *Stratigraphy and Paleoenvironments of the Cretaceous Western Interior Seaway*, edited by W. E. Dean and M. A. Arthur, pp. 127–136, Soc. for Sediment. Geol., Tulsa, Okla.

Schlanger, S. O., and H. C. Jenkyns (1976), Cretaceous oceanic anoxic events: Causes and consequences, *Geol. Mijnbouw*, *55*, 179–184.

Schlanger, S. O., M. A. Arthur, H. C. Jenkyns, and P. A. Scholle (1987), The Cenomanian-Turonian oceanic anoxic event, I. Stratigraphy and distribution of organic carbon-rich beds and the marine $\delta^{13}C$ excursion, in *Marine Petroleum Source Rocks*, edited by J. Brooks and A. J. Fleet, pp. 371–399, Geol. Soc. of London, London.

Scholle, P. A., and M. A. Arthur (1980), Carbon isotope fluctuations in Cretaceous pelagic limestones: Potential stratigraphic and petroleum exploration tool, *AAPG Bull.*, *64*, 67–87.

Schouten, S., E. C. Hopmans, A. Forster, Y. van Breugel, M. M. M. Kuypers, and J. S. Sinninghe Damsté (2003), Extremely high sea-surface temperatures at low latitudes during the middle Cretaceous as revealed by archaeal membrane lipids, *Geology*, *31*, 1069–1072.

Sinninghe Damsté, J. S., and J. W. de Leeuw (1990), Analysis, structure and geochemical significance of organically-bound sulphur in the geosphere: State of the art and future research, *Org. Geochem.*, *16*, 1077–1101.

Sinninghe Damsté, J. S., T. I. Eglinton, J. W. De Leeuw, and P. A. Schenck (1989a), Organic sulphur in macromolecular sedimentary organic matter I. Structure and origin of sulphur-containing moieties in kerogen, asphaltenes and coals as revealed by flash pyrolysis, *Geochem. Cosmochim. Acta*, *53*, 873–899.

Sinninghe Damsté, J. S., W. I. C. Rijpstra, A. C. Kock-van Dalen, J. W. de Leeuw, and P. A. Schenck (1989b), Quenching of labile functionalized lipids by inorganic sulphur species: Evidence for the formation of sedimentary organic sulphur compounds at the early stages of diagenesis, *Geochem. Cosmochim. Acta.*, *53*, 1343–1355.

Sinton, C. W., and R. A. Duncan (1997), Potential links between ocean plateau volcanism and global ocean anoxia at the Cenomanian-Turonian boundary, *Econ. Geol.*, *92*, 836–842.

Slomp, C. P., S. J. Van der Gaast, and W. Van Raaphorst (1996), Phosphorous binding by poorly crystalline iron oxides in North Sea sediments, *Mar. Chem.*, *52*, 55–73.

Snow, L. J., R. A. Duncan, and T. J. Bralower (2005), Trace element abundances in the Rock Canyon Anticline, Pueblo, Colorado, marine sedimentary section and their relationship to Caribbean plateau construction and oxygen anoxic event 2, *Paleoceanography*, *20*, PA3005, doi:10.1029/2004PA001093.

Tappan, H., and A. R. Loeblich (1973), Evolution of the ocean plankton, *Earth Sci. Rev.*, *9*, 207–240.

Thamdrup, B., and D. E. Canfield (1996), Pathways of carbon oxidation in continental margin sediments off central Chile, *Limnol. Oceanogr.*, *41*, 1629–1650.

Tortell, P. D., M. T. Maldonado, and N. M. Price (1996), The role of heterotrophic bacteria in iron-limited ocean ecosystems, *Nature*, *383*, 330–332.

Toth, D. J., and A. Lerman (1977), Organic matter reactivity and sedimentation rates in the ocean, *Am. J. Sci.*, *277*, 465–485.

Tsikos, H., et al. (2004), Carbon-isotope stratigraphy recorded by the Cenomanian–Turonian oceanic anoxic event: Correlation and implications based on three key localities, *J. Geol. Soc. London*, *161*, 711–719.

Turekian, K. K., and K. H. Wedepohl (1961), Distribution of the elements in some major units of the Earth's crust, *Geol. Soc. Am. Bull.*, *72*, 175–192.

Van Cappellen, P., and E. D. Ingall (1994), Benthic phosphorous regeneration, net primary production, and ocean anoxia: A model of the coupled marine biogeochemical cycles of carbon and phosphorous, *Paleoceanography*, *9*, 677–692.

Vismann, B. (1990), Sulfide detoxification and tolerance in *Nereis (Hediste) diversicolor* and *Nereis (Neanthes) virens* (Annelida: Polychaeta), *Mar. Ecol. Prog. Ser.*, *59*, 229–238.

Vorlicek, T. P., and G. R. Helz (2002), Catalysis by mineral surfaces: Implications for Mo geochemistry in anoxic environments, *Geochim. Cosmochim. Acta.*, *66*, 3679–3692.

Wang, F., and P. M. Chapman (1999), Biological implications of sulfide in sediment—A review focusing on sediment toxicity, *Environ. Toxicol. Chem.*, *18*, 2526–2532.

Werne, J. P., D. J. Hollander, A. Behrens, P. Schaeffer, P. Albrecht, and J. S. Sinninghe Damsté (2000), Timing of early diagenetic sulfurization of organic matter: A precursor-product relationship in Holocene sediments of the anoxic Cariaco Basin, Venezuela, *Geochem. Cosmochim. Acta*, *64*, 1741–1751.

Werne, J. P., B. B. Sageman, T. W. Lyons, and D. J. Hollander (2002), An integrated assessment of a "type euxinic" deposit: Evidence for multiple controls on black shale deposition in the middle Devonian Oatka Creek Formation, *Am. J. Sci.*, *302*, 110–143.

Westrich, J. T., and R. A. Berner (1984), The role of sedimentary organic matter in bacterial sulfate reduction: The G model tested, *Limnol. Oceanogr.*, *29*, 236–249.

Wijsman, J. W. M., J. J. Middelburg, and C. H. R. Heip (2001), Reactive iron in Black Sea sediments: Implications for iron cycling, *Mar. Geol.*, *172*, 167–180.

Wu, J., E. Boyle, W. Sundra, and L.-S. Wen (2001), Soluble and colloidal iron in the oligotrophic North Atlantic and North Pacific, *Science*, *293*, 847–849.

Zheng, Y., R. F. Anderson, A. van Geen, and J. Kuwabara (2000), Authigenic molybdenum formation in marine sediments: A link to pore water sulfide in the Santa Barbara Basin, *Geochim. Cosmochim. Acta*, *64*, 4165–4178.

————————————

S. R. Meyers, Department of Geological Sciences, University of North Carolina at Chapel Hill, Chapel Hill, NC 27599-3315, USA. (smeyers@email.unc.edu)